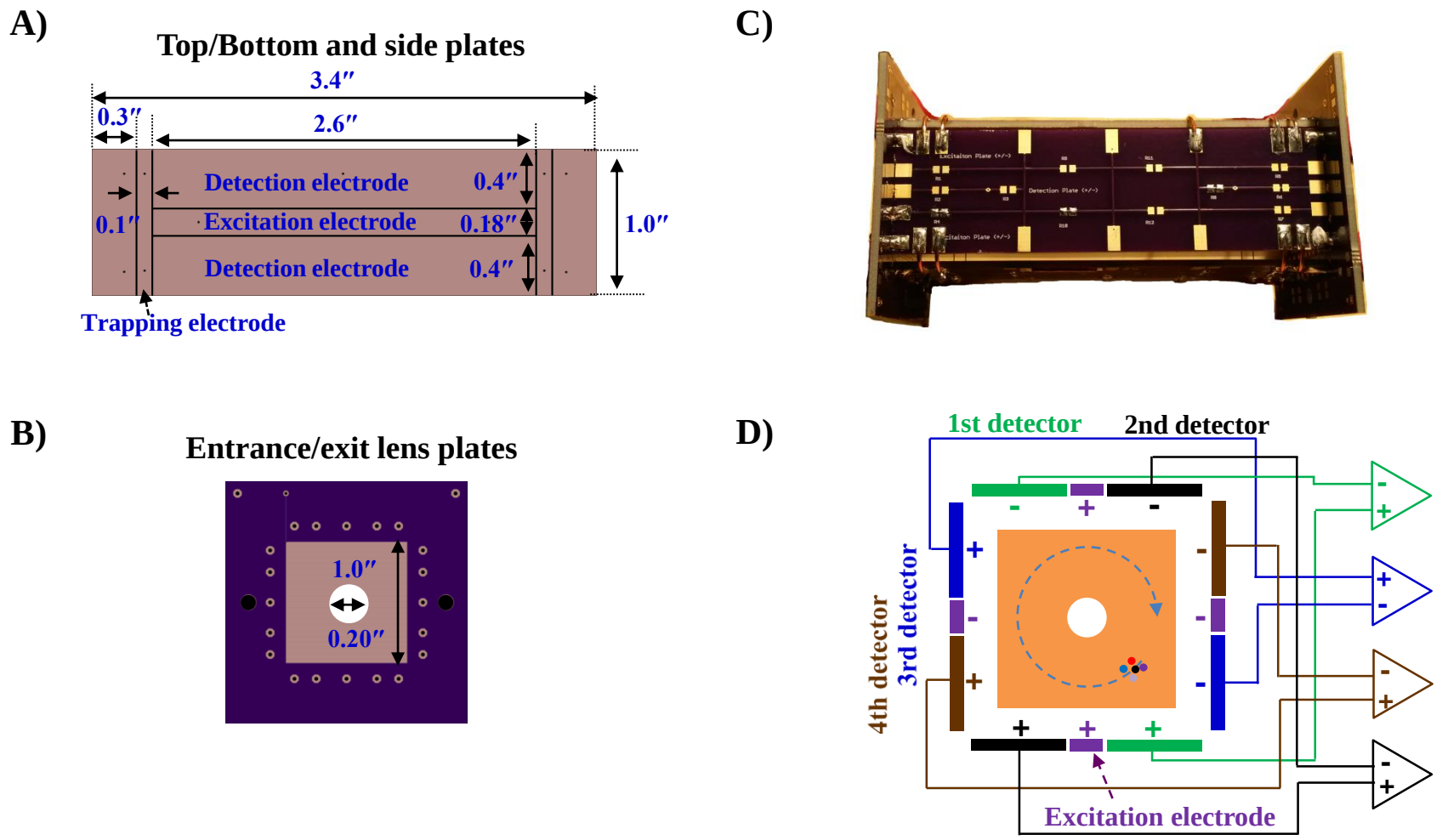

Figure 1. Individual PCB components and an ICR cell with 4 pairs of dipole detection electrodes. Top/bottom and side **(A)** plates showing excitation, detection and trapping electrodes printed on board. Entrance/exit lens plates **(B)**. The assembled ICR cell with 4 pairs of dipole detection electrodes **(C)** and the transverse cross section (magnetic field axis projects into the plane of this figure) with a wiring diagram **(D)**.

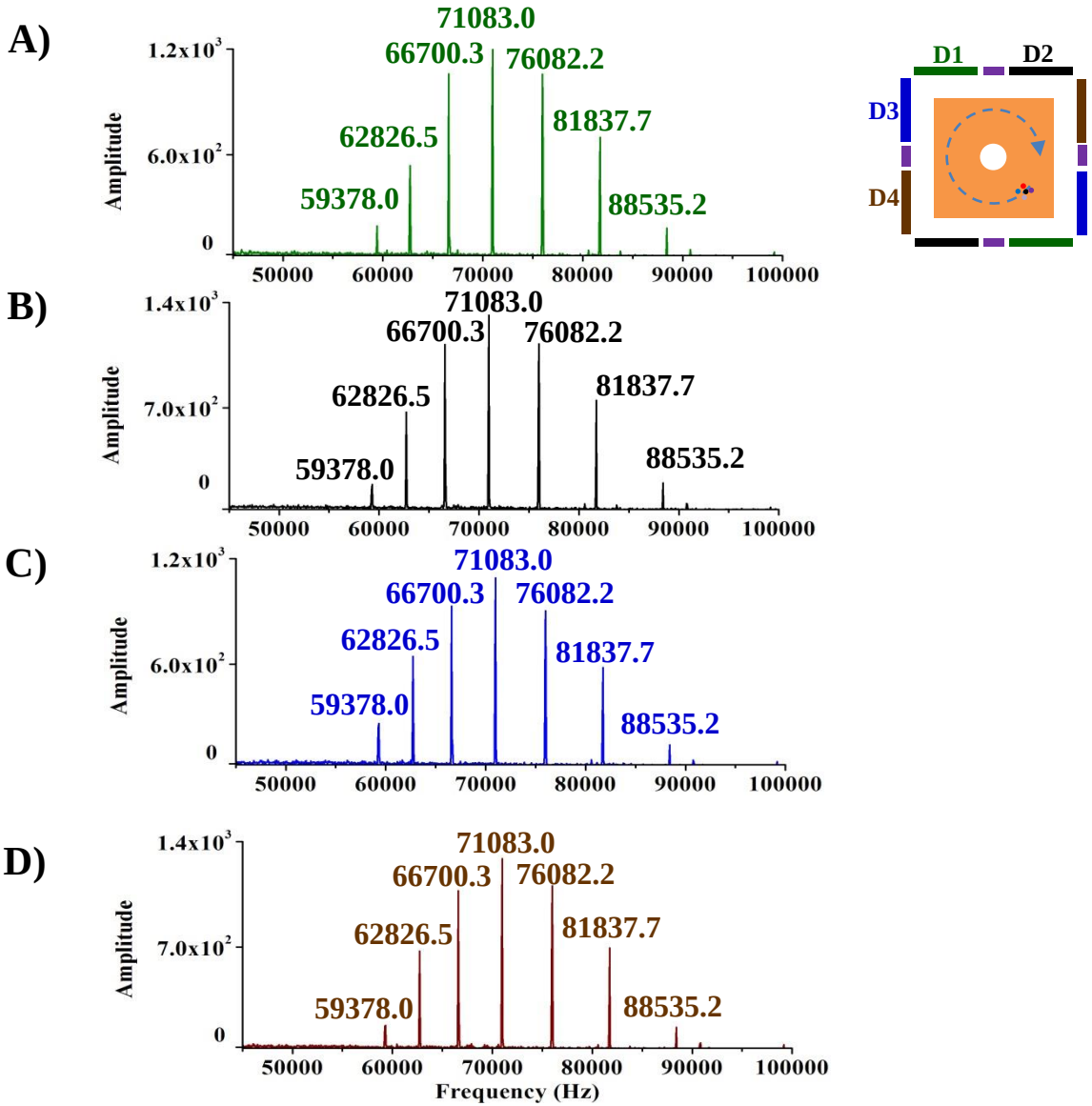

Figure 2. Parallel frequency-domain spectra obtained from detector pair 1 (**A**), detector pair 2 (**B**), detector pair 3 (**C**) and detector pair 4 (**D**) in a single ICR cell at the same time using Ultramark 1621.

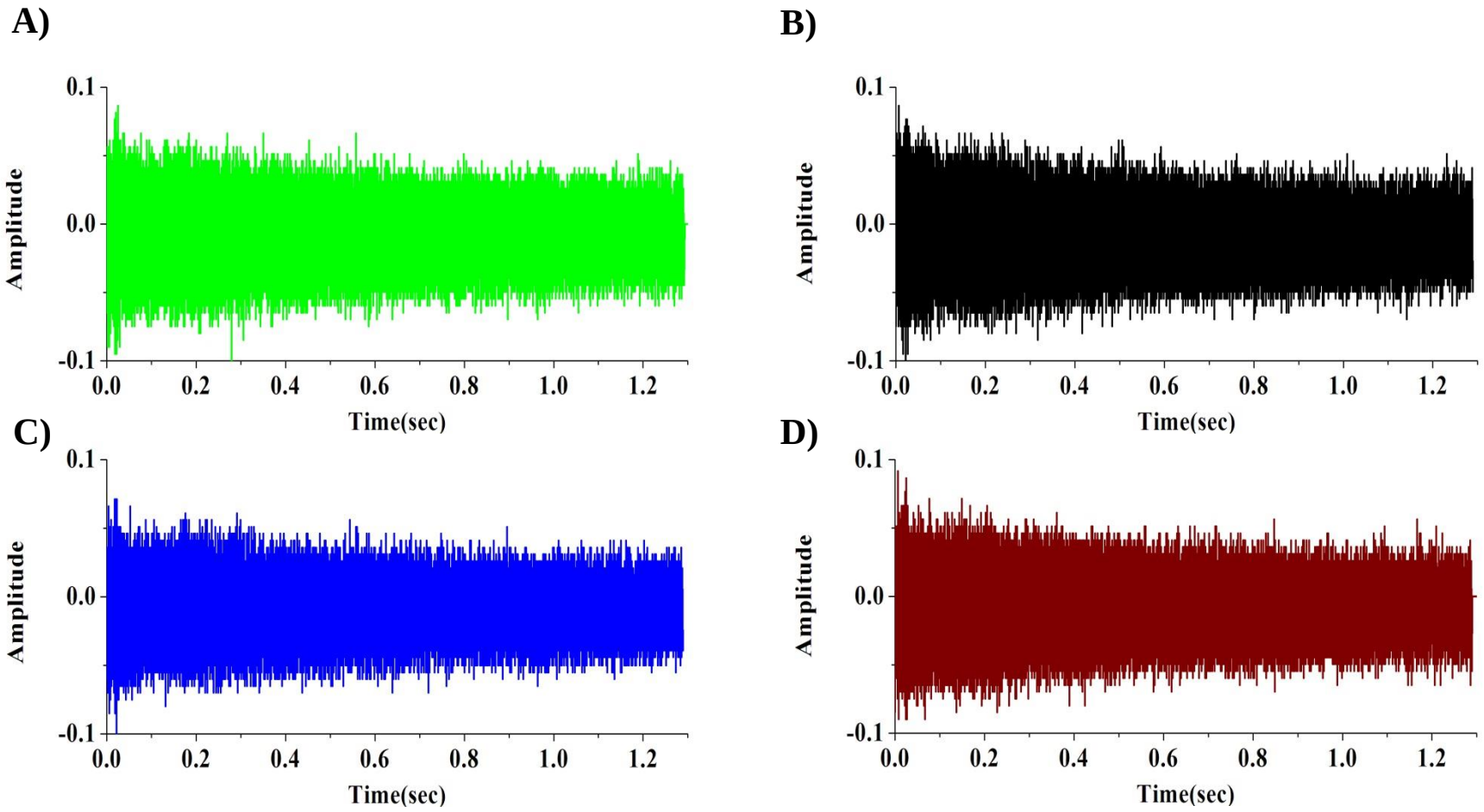

Figure 3. Parallel time domain signals (transients) from detector pair 1 (**A**), detector pair 2 (**B**), detector pair 3 (**C**) and detector pair 4 (**D**) in a single ICR cell at the same time using Ultramark 1621.

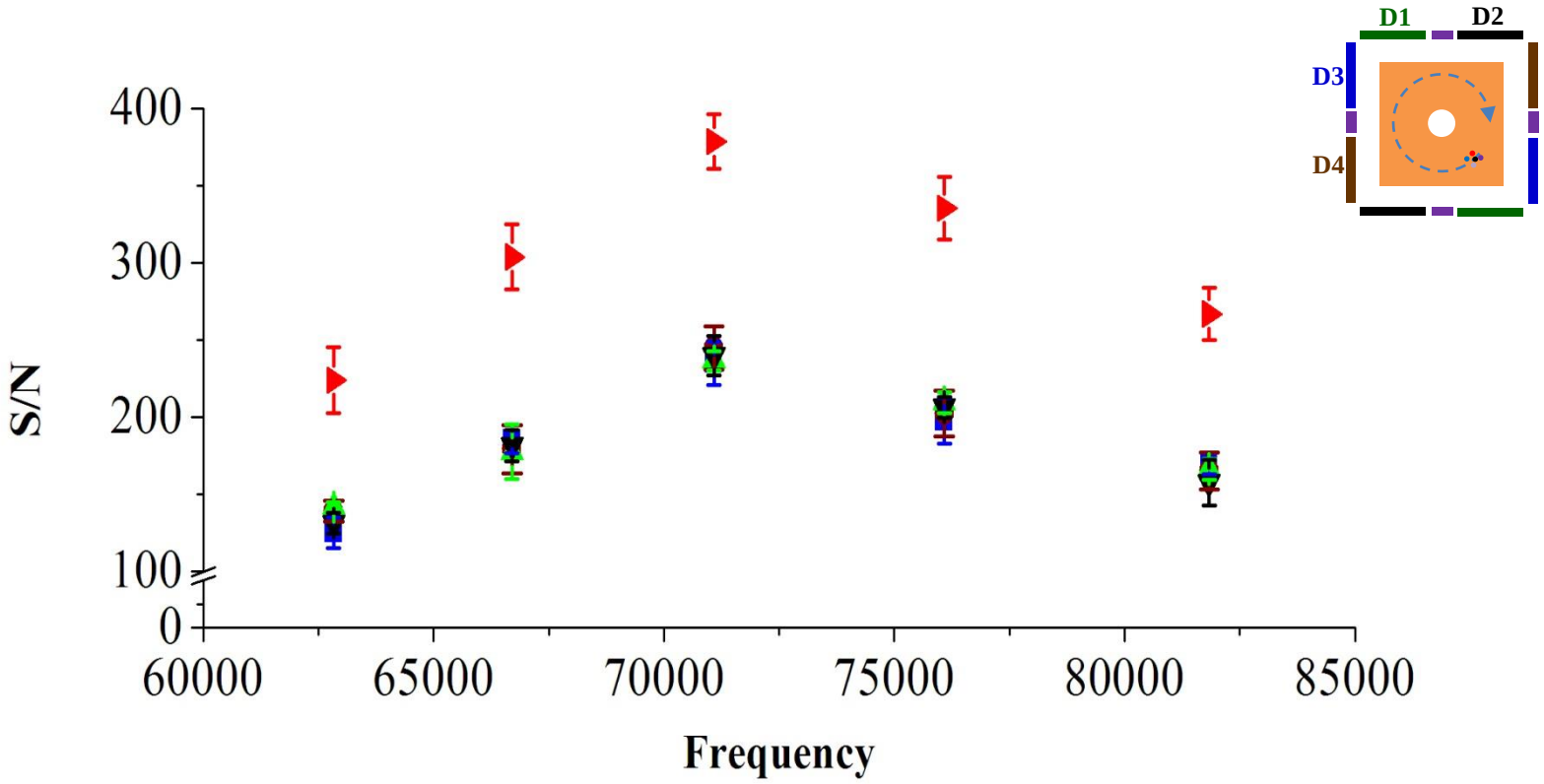

Figure 4. S/N for all peaks observed in the parallel frequency-domain spectra from the detector pairs 1(▲), 2(▼), 3(■) and 4 (●), and all peaks observed in the frequency spectrum (►) from summing the parallel frequency spectra.

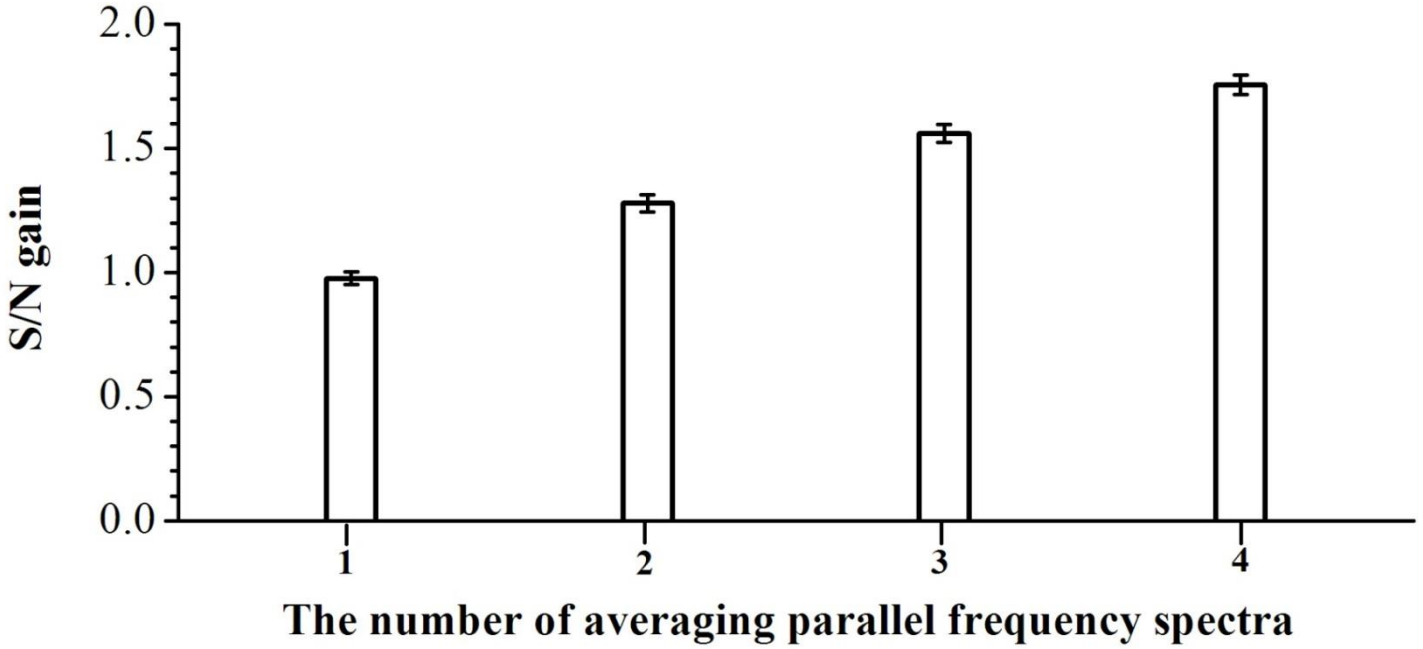

Figure 5. Averaged S/N gains as a function of the number of dipole detection electrodes. The averaged S/N gains were obtained from averaging S/N for all peaks

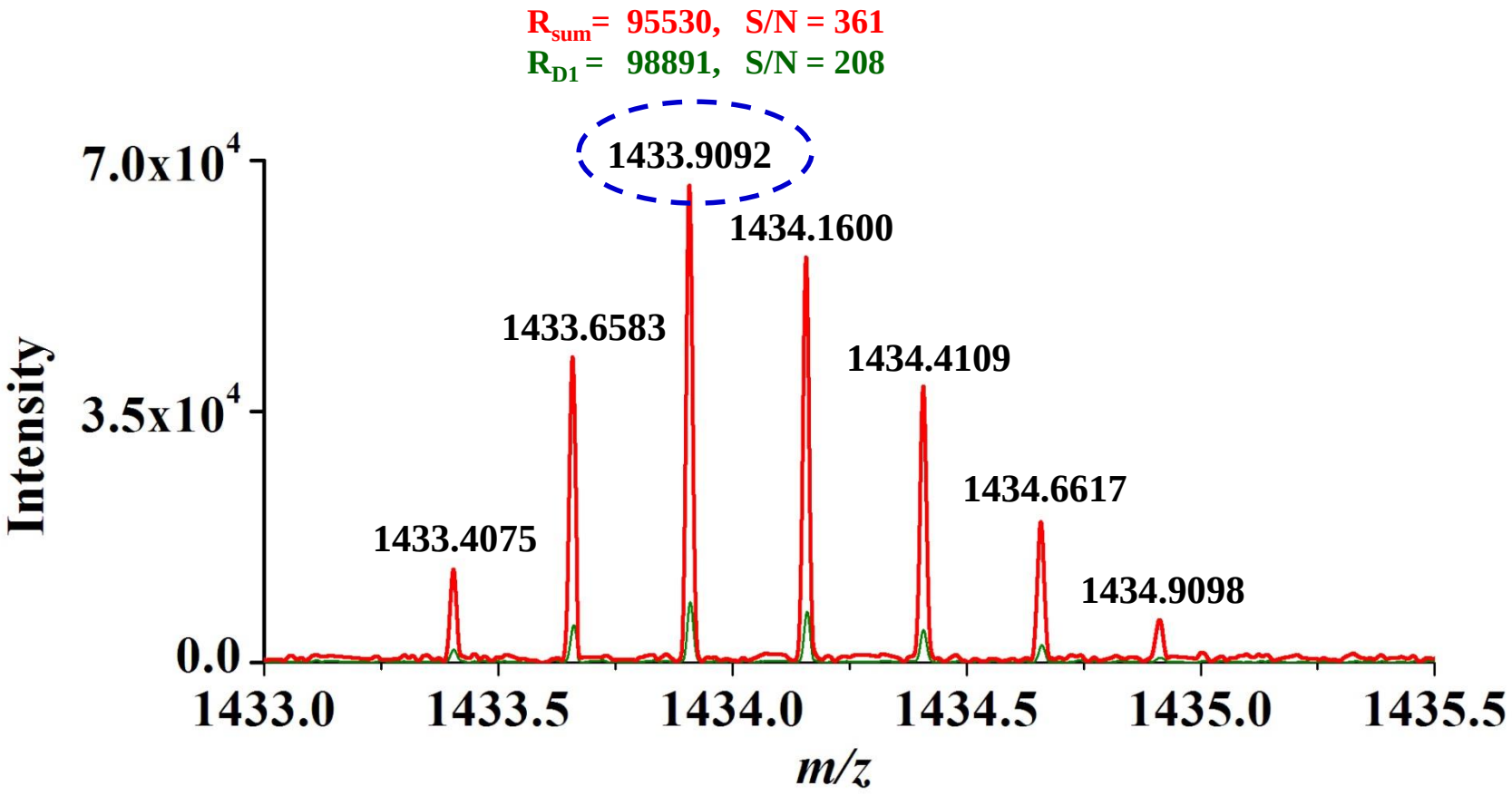

Figure 6. Mass spectra of +3 charged insulin ion showing resolving power R (fwhm) of nearly 100,000 . $\mathbf{R_{D1}}$ and $\mathbf{R_{sum}}$ are resolving power for the peaks observed in the mass spectrum from detector pair 1 and the new mass spectrum from summing the 4 parallel spectra.